Desert Hedgehog-Driven Endothelium Integrity Is Enhanced by Gas1 (Growth Arrest-Specific 1) but Negatively Regulated by Cdon (Cell Adhesion Molecule-Related/Downregulated by Oncogenes)

Candice Chapouly, Pierre-Louis Hollier, Sarah Guimbal, Lauriane Cornuault, Alain-Pierre Gadeau, Marie-Ange Renault

▶ **To cite this version:**

Candice Chapouly, Pierre-Louis Hollier, Sarah Guimbal, Lauriane Cornuault, Alain-Pierre Gadeau, et al.. Desert Hedgehog-Driven Endothelium Integrity Is Enhanced by Gas1 (Growth Arrest-Specific 1) but Negatively Regulated by Cdon (Cell Adhesion Molecule-Related/Downregulated by Oncogenes). Arteriosclerosis, Thrombosis, and Vascular Biology, 2020, ATVBAHA120314441, Online ahead of print. 10.1161/ATVBAHA.120.314441 . inserm-02983021

HAL Id: inserm-02983021

https://inserm.hal.science/inserm-02983021v1

Submitted on 29 Oct 2020

HAL is a multi-disciplinary open access archive for the deposit and dissemination of scientific research documents, whether they are published or not. The documents may come from teaching and research institutions in France or abroad, or from public or private research centers.

L'archive ouverte pluridisciplinaire **HAL**, est destinée au dépôt et à la diffusion de documents scientifiques de niveau recherche, publiés ou non, émanant des établissements d'enseignement et de recherche français ou étrangers, des laboratoires publics ou privés.

Desert Hedgehog-driven endothelium integrity is enhanced by Gas1 but negatively regulated by Cdon

Authors and affiliations
Candice Chapouly[1], Pierre-Louis Hollier[1], Sarah Guimbal[1], Lauriane Cornuault[1], Alain-Pierre Gadeau[1] and Marie-Ange Renault[1]

[1] Univ. Bordeaux, Inserm, Biology of Cardiovascular Diseases, U1034, F-33604 Pessac, France

Short title
Gas1 and Cdon modulate Dhh effects in ECs

Corresponding author
Marie-Ange Renault
Inserm U1034
1, avenue de Magellan
33604 Pessac
France
e-mail : marie-ange.renault@inserm.fr
Tel : (33) 5 57 89 19 79

Keywords: Endothelial cells, vascular integrity, Hedgehog signaling, co-receptors

Subject terms: Basic Science Research, Angiogenesis, Vascular Biology, Blood-Brain Barrier, Cell Signaling/Signal Transduction

Word count: 7206

Total number of Figures: 6
TOC category: Basic Science Research

TOC subcategory: Vascular Biology

Abstract

Evidences accumulated within the past decades, identified Hedgehog (Hh) signaling as a new regulator of endothelium integrity. More specifically, we recently identified Desert Hedgehog (Dhh) as a downstream effector of Klf2 in endothelial cells (ECs). **Objective**: The purpose of this study is to investigate whether Hh co-receptors Gas1 and Cdon may be used as therapeutic targets to modulate Dhh signaling in ECs. **Approach and results**: We demonstrated that both Gas1 and Cdon are expressed in adult ECs and relied on either siRNAs or EC specific conditional KO mice to investigate their role. We found that Gas1 deficiency mainly phenocopies Dhh deficiency especially by inducing VCAM-1 and ICAM-1 overexpression while Cdon deficiency has opposite effects by promoting endothelial junction integrity. At a molecular level, Cdon prevents Dhh binding to Ptch1 and thus acts a decoy receptor for Dhh, while Gas1 promotes Dhh binding to Smo and as a result potentiates Dhh effects. Since Cdon is upregulated in ECs treated by inflammatory cytokines including TNFα and Il1β, we then tested whether Cdon inhibition would promote endothelium integrity in acute inflammatory conditions and found that both fibrinogen and IgG extravasation were decreased in association with an increased Cdh5 expression in the brain cortex of EC specific Cdon KO mice administered locally with Il1β. **Conclusions:** Altogether these results demonstrate that Gas1 is a positive regulator of Dhh in ECs while Cdon is a negative regulator. Interestingly Cdon blocking molecules may then be used to promote endothelium integrity, at least in inflammatory conditions.

Abbreviations

Hh: Hedgehog

Dhh: Desert Hedgehog

Shh: Sonic Hedgehog

FL-Dhh: Full length Desert Hedgehog

EC: endothelial cell

Klf2: Kruppel Like Factor 2

Il1β: Interleukin-1 beta

TNFα: Tumor necrosis factor alpha

Gas1: Growth Arrest Specific 1

Cdon: Cell adhesion molecule-related/down-regulated by oncogenes

Cdh5: Cadherin-5 or Vascular endothelial cadherin

ICAM-1: Intercellular Adhesion Molecule 1

VCAM-1: Vascular Cell Adhesion Molecule 1

Smo: Smoothened

Ptch1: Patched-1

HUVEC: Human umbilical vein endothelial cell

HMVEC-D: Human dermal microvascular endothelial cell

HBMEC: Human brain microvascular endothelial cell

IP: immunoprecipitation

NF-κB: Nuclear factor-kappa B

MTT: Methyl thiazolyl tetrazolium

Introduction

Endothelium integrity i.e. preserved endothelial anatomical structure and function is essential to vascular homeostasis, since a failure of this system represents a critical factor in cardiovascular and cerebrovascular disease pathogenesis. Indeed, the endothelium is involved in many physiological processes such as regulation of vascular permeability, vascular tone, blood coagulation as well as homing of immune cells to specific sites of the body. Conversely, endothelial dysfunction is associated with excessive vasoconstriction especially because of impaired endothelial nitric oxide production. Also, endothelial dysfunction is characterized by abnormal vascular leakage due to altered endothelial intercellular junctions. Finally, dysfunctional endothelial cells (ECs) acquire pro-inflammatory and pro-thrombotic phenotypes by expressing increased levels of adhesion and pro-thrombotic molecules such as vascular cell adhesion molecule-1 (VCAM-1) and intercellular adhesion molecule-1 (ICAM-1) [1].

Evidences accumulated within the past decades, identified Hedgehog (Hh) signaling as a new regulator of endothelium integrity [2]. For instance, Hh signaling was shown to promote blood brain barrier integrity and immune quiescence both in the setting of multiple sclerosis [3] and in the setting of stroke [4]. Additionally we have shown that disruption of Hh signaling specifically in ECs induces blood-nerve barrier breakdown and peripheral nerve inflammation [5]. While investigating molecular mechanisms underlying Hh regulation of endothelium integrity, we found that Desert Hedgehog (Dhh) is the main Hh ligand express by ECs [6,7]. Of note, Indian Hedgehog (Ihh) was reported to be expressed in some specific vascular bed including the one of the eye choroid [8,9] while Shh is not expressed by ECs [6,7]. Importantly, *Dhh* KO in ECs leads to the disruption of Cadherin-5 (Cdh5)/β-catenin interaction and spontaneous vascular leakage, an increased expression of adhesion molecules including VCAM-1 and ICAM-1 [6] and increased angiogenic capabilities [10]. Besides, Dhh which is upregulated by blood flow and downregulated by inflammatory cytokines, appears to be a downstream effector of the master regulator of endothelial integrity Kruppel like factor 2 (Klf2) [6].

The Hh family of morphogens which includes Sonic hedgehog (Shh), Indian hedgehog and Dhh, was identified nearly 4 decades ago in drosophila as crucial regulators of cell fate determination during embryogenesis [11]. The interaction of Hh proteins with their specific receptor Patched-1 (Ptch1) de-represses the transmembrane protein Smoothened (Smo), which activates downstream pathways, including the Hh canonical pathway leading to the activation of Gli family zinc finger (Gli) transcription factors and so-called Hh non canonical pathways, which are independent of Smo and/or Gli [12].

The Hh ligand binding to Ptch1 is regulated by several coreceptors. Among these, Cell adhesion molecule-related/downregulated by oncogenes (Cdon), Brother of Cdon (Boc) and Growth arrest specific 1 (Gas1) are suggested to promote Hh ligand interaction with Ptch1 while Hedgehog interacting protein (Hhip) inhibits it [13].

Cdon and Boc proteins are cell surface glycoproteins belonging to a subgroup of the Immunoglobulin superfamily of cell adhesion molecules, which also includes the Robo axon-guidance receptors. Their ectodomain respectively contains five and four Ig-like domains, followed by three type III fibronectin (FNIII) repeats (FNIII 1 to 3), a single trans-membrane domain and a divergent intracellular region of variable length [14]. Cdon was shown to interact with all of the three N-terminal active Hh peptides through its third FNIII domain.

Gas1 was identified as one of six genes that were transcriptionally up-regulated in NIH3T3 cells arrested in cell cycle upon serum starvation. *Gas1* encodes a 45-kDa GPI-anchored cell surface protein that binds N-terminal Shh with high affinity [15].
The goal of the present study is to investigate whether Dhh-induced endothelial integrity depends on Hh co-receptors. This is essential to determine whether such co-receptors could be used as therapeutic target to enhance Dhh-induced signaling in ECs under pathological conditions.

Materials and Methods
The authors declare that all supporting data are available within the article and its online supplementary files.

Mice
Cdon Floxed (*Cdon*^{Flox}) mice (Supplemental Figure IA) were generated at the "Institut Clinique de la Souris" through the International Mouse Phenotyping Consortium (IMPC) from a vector generated by the European conditional mice mutagenesis program, EUCOMM. *Cdon* Floxed mice were generated under a C57BL/6N background and backcrossed at least 6 times with C57BL/6J mice before they were used in any experiment. *Gas1*$^{tm3.1Fan}$ (*Gas1*^{Flox}) mice [16(p1)] were kindly given by C.M. Fan. Gas1 Floxed mice were obtained under a 129 background and backcrossed at least 6 times with C57BL/6J mice before they were used in any experiment. Tg(Cdh5-cre/ERT2)1Rha (Cdh5-Cre/ERT2) mice [17] which were a gift from RH. Adams, were obtained and maintained under a C57BL/6J background.
Cdh5-Cre/ERT2 mice were genotyped using the following primers: 5'-TAAAGATATCTCACGTACTGACGGTG-3' and 5'-TCTCTGACCAGAGTCATCCTTAGC-3' that amplify 493 bp of the Cre recombinase sequence. Cdon Floxed mice were genotyped using the following primers 5'- CTTCCCAGAGGGTGTGAGAGCAATG-3' and 5'-GAACCAGTAGCATGCATGATGCTGG-3' which amplifies a 385 bp fragment of the WT allele or a 494 bp fragment if the allele is floxed. *Gas1* Floxed mice were genotyped using the following primers 5'-GAATCGAAGCGCCTGGACC-3' and 5'-GGAAAACCGCACAGAAGAGGG-3' which amplifies a 285 bp fragment of the WT allele or a 360 bp fragment if the allele is floxed.
Animal experiments were performed in accordance with the guidelines from Directive 2010/63/EU of the European Parliament on the protection of animals used for scientific purposes and approved by the local Animal Care and Use Committee of Bordeaux University.
The Cre recombinase in Cdh5-Cre/ERT2 mice was activated by intraperitoneal injection of 1 mg tamoxifen for 5 consecutive days at 8 weeks of age. Mice were phenotyped 2 weeks later. Successful and specific activation of the Cre recombinase is shown in Supplemental Figure IB-C [6]. Notably, only female were used in both the corneal angiogenesis and Miles assays because male fight and are more likely to have their cornea and back skin injured. Only males were used in the LPS and Ad-Il-1β protocols. At the end of experiments animal were sacrificed via cervical dislocation.

Mouse corneal angiogenesis assay
Pellets were prepared as previously described [18]. Briefly, 5 µg of VEGFA (Shenandoah biotechnology diluted in 10 µL sterile phosphate-buffered saline (PBS) was mixed with 2.5 mg sucrose octasulfate-aluminum complex (Sigma-Aldrich Co., St. Louis, MO, USA), then 10

µL of 12% hydron in ethanol was added. The suspension was deposited on a 400-µm nylon mesh (Sefar America Inc., Depew, NY, USA), then both sides of the mesh were covered with a thin layer of hydron and allowed to dry.
Female mice were anesthetized with an intraperitoneal (IP) injection of ketamine 100 mg/kg and xylazine 10 mg/kg. The eyes of the mice eyes were topically anesthetized with 0.5% Proparacaine™. The globe of the eye was proptosed with jeweler's forceps taking care not to damage the limbus vessel surrounding the base of the globe. Sterile saline was also applied directly to each eye as needed during the procedure to prevent excessive drying of the cornea and to facilitate insertion of the pellet into the lamellar pocket of the eyes. Using an operating microscope, a central, intrasomal linear keratotomy was performed with a surgical blade parallel to the insertion of the lateral rectus muscle. Using a modified von greafe knife, a lamellar micro pocket was made toward the temporal limbus by 'rocking' the von greafe knife back and forth.
VEGFA containing pellet was placed on the cornea surface with jeweler's forceps at the opening of the lamellar pocket. A drop of saline was applied directly to the pellet, and using the modified von greafe knife, the pellet was gently advanced to the temporal end of the pocket. Buprenorphine was given at a dose of 0.05 mg/kg subcutaneously on the day of surgery.
Nine days after pellet implantation, mice were sacrificed, and then eyes were harvested and fixed with 2% paraformaldehyde. Capillaries were stained with rat anti-mouse CD31 antibodies (BMA Biomedicals, Cat#T-2001), primary antibodies were visualized with Alexa 568–conjugated anti-rat antibodies (Invitrogen). Pictures were taken under 50x magnification. Angiogenesis was quantified as the CD31+surface area using Image J software. Notably, such quantification is a rough quantification of angiogenesis, which does not discriminate increased vessel density from increased vessel length. The corneas were given a number at the time of collection, so that pictures were taken blinded and quantifications were done blinded.

In vivo permeability assessment (Miles assay)
The back of female mice was shaved. 72 hours, later mice were administered with 100 µL 1% Evans blue via retro orbital injection. Subsequently they were administered with 50 µL NaCl 0.9% containing or not 20 ng VEGFA (Shenandoah biotechnology) subcutaneously at 6 spots on their back. Buprenorphine was given at a dose of 0.05 mg/kg subcutaneously on the day of surgery.
30 minutes later mice were sacrificed, skin biopsy around each injection point were then harvested to quantify Evans blue extravasation. Evans blue dye was extracted from the skin by incubation at 65°C with formamide. The concentration of Evans blue dye extracted was determined spectrophotometrically at 620 nm with a reference at 740 nm. The genotype of the mice was not known by the experimenter during the entire procedure.

Lipopolysaccharide (LPS) induced systemic inflammation
Mice were administered with 0.05 mg/kg Buprenorphine subcutaneously to avoid any pain. 30 minutes later they were administered with 10 mg/kg LPS (Sigma) intraperitoneally. Finally, mice were sacrificed by cervical dislocation 6 hours after LPS administration, the left lung was harvest, fixed in methanol, paraffin embedded and cut into 7 µm thick sections.
GR1+ cells were quantified after GR1 staining of lung cross sections, using Image J software in 10 pictures taken under 20x magnification. One section per lung was quantified for each

mouse. Lungs were given a number at the time of collection, so that pictures were taken blinded and quantifications were done blinded.

Ad-Il1β stereotaxic injections

Mice were anaesthetized using isoflurane and placed into a stereotactic frame (Stoelting). An ophthalmic *ointment* was applied at the ocular surface to maintain eye hydration during the time of surgery. The skull was shaved and the skin incised on 1 cm to expose the skull cap. Then, a hole was drilled into the cerebral cortex and 3 µL of an AdIl-1β [19] or AdDL70 control (AdCtrl), (10^7 pfu) solution was microinjected at y=1 mm caudal to Bregma, x=2 mm, z=1.5 mm using a Hamilton syringe, into the cerebral cortex and infused for 3 minutes before removing the needle from the skull hole [20]. Mice received a subcutaneous injection of buprenorphine (0.05 mg/kg) 30 minutes before surgery and again 8 hours post-surgery to assure a constant analgesia during the procedure and postoperatively. Mice were sacrificed 7 days post-surgery. For histological assessment, brains were harvested and fixed in formalin for 3 hours before being incubated in 30% sucrose overnight and OCT embedded. Then, for each brain, the lesion area identified by the puncture site was cut into 7 µm thick sections.

BBB permeability was evaluated by measuring tight junction integrity and plasmatic protein extravasation. For each brain Cdh5+, Fibrinogen+, IgG+ areas were quantified, using Image J software, in 20 pictures taken at the margins of the lesion area under 40x magnification. CD45+ leukocytes were counted in 20 pictures randomly taken under 40x magnification. CD11b+, Gfap+ and NeuN+ areas were quantified in 10 pictures taken in and around the lesion area under 20X magnification. One section, localized in the Il-1β-induced inflammatory lesion area, per brain was quantified for each mouse. Brains were given a number at the time of collection, so that pictures were taken blinded and quantifications were done blinded.

Immunostaining

Prior to staining, whole mount corneas were fixed with 2.5% formaline for 10 minutes, brain were fixed with 10% formaline for 3 hours, heart and lungs were fixed with methanol for 24 hours and cultured cells were fixed with 10% formaline for 10 minutes.

Capillaries were identified using rat anti-mouse CD31 antibodies (BMA Biomedicals, Cat#T-2001). Neutrophils were stained with rat anti-Ly6G (GR1) antibodies (BD Pharmingen Inc, Cat#551459). Human Cdh5 was stained using mouse anti-human Cdh5 antibodies (Santa Cruz Biotechnology, Inc, Cat#sc-9989). Mouse Cdh5 was stained using goat anti-mouse Cdh5 antibodies (R&D systems, Cat# AF1002). Albumin and fibrinogen were stained using sheep anti-albumin antibodies (Abcam, Cat# ab8940) and rabbit anti-fibrinogen antibodies (Dako, Cat#A0080) respectively. Mouse IgGs were stained with Alexa Fluor 568 conjugated donkey anti-mouse IgG (Invitrogen, Cat#A-10037). Pan-leucocytes were identified using rat anti-mouse CD45 antibodies (BD Pharmingen Inc, Cat# 550539). CD11b+ microglia and macrophages were identified using rat anti-CD11b antibodies (Invitrogen, cat#14-0112-82). GFAP was stained using rabbit anti-GFAP antibodies (Invitrogen, Cat# OPA1-06100). Neurons were identified using anti-NeuN antibodies (Millipore, Cat# ABN78). Cdon was stained using goat anti-mouse Cdon antibodies (R&D systems, Cat# AF2429). Gas1 was stained using goat anti-human Gas1 antibodies (R&D systems, Cat# AF2636). Dhh was stained using mouse anti-Dhh antibodies (Santa Cruz Biotechnology, Inc, Cat# sc-271168). Ptch1 was stained using rabbit anti-Ptch1 antibodies (Abcam, Cat# ab53715). For immunofluorescence analyzes, primary antibodies were resolved with Alexa Fluor®–conjugated secondary polyclonal antibodies (Invitrogen, Cat# A-21206, A-21208, A-11077,

A-11057, A-31573, A-10037) and nuclei were counterstained with DAPI (1/5000). For both immunohistochemical and immunofluorescence analyses, negative controls using secondary antibodies only were done to check for antibody specificity.

Cell culture

In vitro experiments were performed using human umbilical vein endothelial cells (HUVECs) (Lonza), human dermal microvascular endothelial cells (HMVECs-D) (Lonza) or human brain microvascular Endothelial Cells (HBMECs) (Alphabioregen). HUVECs and HBMECs were cultured in endothelial basal medium-2 (EBM-2) supplemented with EGM™-2 BulletKits™ (Lonza). HMVECs-D were cultured in endothelial basal medium-2 (EBM-2) supplemented with EGM™-2 MV BulletKits™ (Lonza). Cell from passage 3 to passage 6 were used. Before any treatment cells were serum starved in 0.5% fetal bovine serum medium for 24 hours. HUVECs were cultured in Opti-MEM to perform assays in serum-free conditions. HeLa ATCC®CCL-2™ cells were cultured in Roswell Park Memorial Institute medium (RPMI) supplemented with 10% fetal bovine serum.

Cell culture assays are described in the supplemental method section

Statistics

Results are reported as mean ± SEM. Comparisons between groups were analyzed for significance with the non-parametric Mann-Whitney test or the Kruskal-Wallis test followed by Dunn's multiple comparisons test using GraphPad Prism v8.0.2 (GraphPad Inc, San Diego, Calif). Differences between groups were considered significant when $p \leq 0.05$ (*: $p \leq 0.05$; **: $p \leq 0.01$; ***: $p \leq 0.001$).

Results

ECs express Cdon, Gas1 and Hhip but not Boc.

First, we searched for *Cdon*, *Boc*, *Gas1* and *Hhip* expression in human ECs from different origin, including HUVECs, HMVECs-D and HBMECs via RT-PCR. As shown in Figure 1A, human ECs express *Hhip*, *Cdon*, and *Gas1* mRNA while *Boc* mRNA is express at a lower level. Notably, *Gas1* is not detected in HBMECs. Since the role of endothelial Hhip has already been reported in several papers [21–23], we focused our investigations on Gas1 and Cdon and confirmed their endothelial expression via immunostaining (Figure 1B). Interestingly, while TNFα inhibits *Gas1* mRNA expression in HUVECs (Supplemental Figure IIA), it increases *Cdon* mRNA expression (Supplemental Figure IIB). Notably, TNFα-induced *Cdon* mRNA expression depends on NF-κB activity (Supplemental Figure IIC).

Next, we performed co-immunoprecipitation assays to verify that Dhh is able to bind these receptors. Indeed, Dhh is the main Hh ligand expressed by ECs, especially HUVECs, HMVECs-D and HBMECs (Supplemental Figure IID). While we found that Dhh binds Gas1 directly (Figure 1C), Cdon alone cannot bind Dhh (Figure 1D). However, Dhh can bind Cdon in the presence of Ptch1 (Figure 1E). Consistently, Cdon co-localizes with Dhh only in the presence of Ptch1 while Gas1 co-localizes with Dhh both in the presence and absence of Ptch1. Both Gas1 and Cdon are internalized once they bind Dhh (Supplemental Figure III).

With the aim to investigate the role of Gas1 and Cdon in ECs we performed a series of *in vitro* and *in vivo* assays using siRNAs and EC-specific conditional KO mice respectively.

Cdon promotes EC proliferation, migration and angiogenesis

The role of Gas1 and Cdon in angiogenesis was investigated using the mouse corneal angiogenesis assay. Mice deficient for Gas1 or Cdon expression in EC together with their respective control littermates were implanted with VEGFA containing pellets. While VEGFA-induced angiogenesis was not different in *Gas1*^{ECKO} mice from their control littermates (Figure 2A-B), VEGFA-induced angiogenesis was significantly-inhibited in *Cdon*^{ECKO} mice compared to their control littermates (Figure 2C-D). Consistently, *in vitro* experiments performed in HUVECs showed that both EC proliferation (Figure 2E) and VEGFA-induced EC migration (Figure 2F) were decreased after *Cdon* knock down (KD) (Supplemental Figure IVA). *Gas1* KD (Supplemental Figure IVB) did not modify EC proliferation or VEGFA-induced migration (Figure 2E-F). However, *Gas1* KD did promote EC migration in the absence of VEGFA (Figure 2F).

This set of data demonstrates that Cdon is pro-angiogenic. Notably this effect works in the opposite direction to Dhh anti-angiogenic effect [10].

Gas1 prevent EC activation and LPS-induced neutrophil recruitment.

To investigate the role of Gas1 and Cdon in regulating EC immune quiescence, HUVECs were transfected with *Gas1*, *Cdon* or control siRNAs. VCAM-1 and ICAM-1 expression was measured via both RT-qPCR and western blot analyses. While *Gas1* KD significantly increased both VCAM-1 and ICAM-1 expression, *Cdon* KD did not (Figure 3A-C). These results were confirmed in TNFα-treated cells (Figure 3D-E). Finally, to assess the functional consequences of EC activation *in vivo*, we quantified neutrophils recruitment in the lungs of mice that were administered with LPS. As expected, neutrophil density in the lung of *Gas1*^{ECKO} mice was significantly increased (Figure 3F-G) compared to their control littermates while we found no difference between *Cdon*^{ECKO} mice and control littermates (Figure 3H-I).

Altogether these data demonstrate that Gas1 prevents EC activation similarly to Dhh [6]. On the contrary, Cdon does not seem to participate in the regulation of EC activation.

Cdon disrupts adherens junction integrity.

The role of Gas1 and Cdon in controlling endothelial intercellular junction integrity was first investigated *in vitro*. HUVECs were transfected with *Gas1*, *Cdon* or control siRNAs. Adherens junction integrity was quantified after Cdh5 immunostaining (Figure 4A) and endothelium permeability using Transwells. We found that *Gas1* KD disrupts Cdh5-dependent junction integrity (Cdh5 junctions acquire a thicker, nonlinear phenotype) (Figure 4B) while *Cdon* KD prevents EC permeability (Figure 4C). *Gas1* KD did not show any effects in the permeability assay test. Indeed, Endothelial Cdh5 junction may have a nonlinear phenotype but still be continuous [24]. Consistently, in the Miles assay *in vivo,* VEGFA-induced vascular permeability was not different between *Gas1*^{ECKO} and control mice (Figure 4D) while it was decreased in the absence of endothelial Cdon (Figure 4E). This last set of data demonstrate that Cdon strongly increases vascular permeability unlike Dhh [6,10] and that Gas1 may slightly modify Cdh5 junction organization without functional consequences.

To conclude on this first set of results, Gas1 may promote Hh signaling in ECs since Gas1 KD mostly recapitulates the effects of *Dhh* KD. On the contrary, Cdon most likely inhibits Hh signaling since *Cdon* KD induces opposite effect to those of *Dhh* KD. Notably, Cdon has been previously identified as a Hh decoy receptor in the zebrafish optic vesicle [25].

Therefore, in the second part of this study, we chose to perform a series of experiments aiming to investigate whether and how Gas1 and Cdon modulate Hh signaling in ECs.

Gas1 promotes Dhh interaction with Smo while Cdon prevents Dhh interaction with Ptch1.

First, we tested whether Gas1 or Cdon modulate Dhh interaction with Ptch1 and Smo. Notably, Smo has been recently shown to be a receptor for Hh ligands especially in the case of cell autonomous signaling [26]. Interestingly, we found that Gas1 prevents Dhh interaction with Ptch1 but promotes Dhh interaction with Smo. On the contrary, Cdon prevents Dhh interaction with Ptch1 but does not modify Dhh interaction with Smo (Figure 5A-B).

Since *Gas1* KD phenocopies most features of *Dhh* deficiency, we tested whether Gas1 effects on endothelial adherens junction's integrity and migration depend on Hh signaling. To do so, we performed rescue experiments. HUVECs were either transfected with *Gas1* or control siRNAs and then treated or not with the Smo agonist SAG. As shown in Supplemental Figure IVC-D, *Gas1* KD-induced Cdh5 junction thickening was prevented in the presence of SAG. Similarly, *Gas1* KD failed to induce EC migration in the presence of SAG (Supplemental Figure IVE). However, SAG had no effect on *Gas1* KD-induced VCAM-1 and ICAM-1 (Supplemental Figure IVF and IVG). Notably, VCAM-1 and ICAM-1 seem to be downstream of Ptch1 rather than Smo since *Ptch1* KD is sufficient to increase their expression (Supplemental Figure IVH-J).

Because Cdon has opposite effects to Dhh ones, we hypothesized that Cdon is a decoy receptor for Dhh at the surface of EC and thus tested whether si*Cdon*-induced effects are prevented in the absence of Dhh. HUVECs were transfected with *Cdon* siRNAs alone or in combination with *Dhh* siRNAs. While si*Cdon* alone decreased adherens junction thickness and endothelium permeability, in the si*Cdon* + si*Dhh* condition, effects were no longer significant (Figure 5 D-F) confirming our hypothesis. Beside, we verified whether si*Cdon* still decrease endothelium permeability in the absence of serum (Figure 5G), confirming that Cdon does improve endothelial junction integrity not by interfering with any circulating Hh ligands but rather by interfering with EC-derived Dhh.

Cdon deficiency at the endothelium prevents blood-brain barrier opening in the setting of acute inflammation

Finally, since Cdon appears to act as a negative regulator of Dhh-induced signaling in ECs, we hypothesized that blocking Cdon may promote Dhh-induced signaling in ECs and subsequently promote maintenance of endothelium integrity in pathological conditions.

To test such hypothesis, we administered adenoviruses encoding Il-1β locally in the cortex of both $Cdon^{ECKO}$ mice and their control littermate to induce acute brain inflammation and BBB breakdown.

Notably, Cdon expression is significantly increased upon Il-1β treatment in both HUVECs and HBMECs (Figure 6A-B). In accordance with our hypothesis, endothelial adherens junctions were preserved in the absence of Cdon, as attested by an increased Cdh5 expression in the cortical lesion area of $Cdon^{ECKO}$ mice injected with Il-1β, compared to control littermates (Figure 6C-D). Consistently, both fibrinogen and IgG extravasation were decreased (Figure 6C, E-F). BBB tightness in $Cdon^{ECKO}$ mice was associated with a decreased leucocyte infiltration, a decreased microglia and astrocyte activation and finally with an increased neuron survival (Supplemental figure VA-E).

These last results demonstrate that blocking Cdon might indeed be a working therapeutic strategy to preserve endothelium integrity in pathological setting such as acute neuro-inflammation.

Cdon blocking antibodies may be used as a therapeutic tool to maintain endothelial junctions in the setting of inflammation

We then tested whether Cdon antibodies may be used as a therapeutic tool to block Dhh binding to Cdon and improve endothelial integrity. To do so, HUVECs were treated or not with TNFα, in the presence or not of Cdon blocking antibodies. As shown in Figure 6G-H, TNFα-induced Cdh5 junction thickening is prevented in the presence of Cdon blocking antibodies.

Discussion

Hh signaling has been described to be regulated by several co-receptors including Hhip, Boc, Cdon and Gas1 especially in the setting of embryogenesis [27]. The purpose of the present study was to investigate the role of Gas1 and Cdon in ECs in adults. Importantly, Hh signaling in ECs is original by several aspects. First, it exclusively involves non canonical signaling [28,29], second, it is activated by full length unprocessed Dhh (FL-Dhh) [10] and third, it occurs cell autonomously [6]. It is important to have in mind that full length unprocessed Hh ligands, may not only bind Ptch1 but also Smo directly [26]. In this particular setting, the present study demonstrates that Cdon prevents FL-Dhh binding to Ptch1. Gas1 also prevents FL-Dhh binding to Ptch1 but promotes FL-Dhh binding to Smo. By doing so, Cdon mainly acts as a negative regulator of FL-Dhh and destabilizes EC junctions to promote angiogenesis while Gas 1 is a positive regulator of FL-Dhh which prevents EC activation (Supplemental Figure VI).

Cdon, Gas1 and Boc are typically believed to be positive regulators of Hh signaling [13] in line with the fact that Gas1, Cdon and Boc were shown to be equally capable of promoting Shh signaling during neural patterning since overexpression of any individual component results in ectopic ventral cell fate specification [27]. Additionally, while genetic removal of Gas1, Cdon or Boc individually has only modest effects on Shh signaling, removal of any two components results in significantly reduced Shh-dependent ventral neural patterning [27]. However, conflicting results have been published: Gas1 was first shown to bind Shh in 2001. In this study, it was suggested to reduce the availability of active Shh in the somite based on ectopic expression studies [30]. In 2007, experiments using *Gas1* deficient mice revealed, on the contrary, that Gas1 is a positive regulator of Shh signaling and facilitates Shh low level effects [31]. Similarly, Cdon was shown to positively regulate Shh-induced signaling especially in the developing brain [32,33] while it was more recently shown to act as a Hh decoy receptor during proximal-distal patterning of the optic vesicle [25]. Whether Gas1 and Cdon are positive or negative regulators of Hh signaling may then most likely depend on the type of ligand and cell type involved.

Hh signaling in ECs is still far from being fully understood [2]. We have previously shown that Dhh prevents EC activation by downregulating VCAM-1 and ICAM-1 and protects adherens junction integrity by promoting Cdh5 interaction with β-catenin [6]. The present study suggests that Dhh regulates EC activation and EC junction integrity via distinct pathways. Indeed, while Cdon mainly affects Dhh regulation of endothelial junctions, Gas1 mainly regulates Dhh regulation of EC immune quiescence. In both cases, a dialogue between Ptch1 and Smo

seems to be involved, since Cdon modulates Dhh interaction with Ptch1 to regulate EC junctions, while we previously found that Cdh5 junction integrity depends on Smo [10]. Similarly, Gas1 promotes Dhh binding with Smo to prevent EC activation, while we found that *Ptch1* KD is sufficient to increase VCAM-1 and ICAM-1 expression in ECs. We then hypothesized that both dialogues going from Ptch1 to Smo and Smo to Ptch1 exist (Supplemental Figure VI) based on the reciprocal regulation of Ptch1 and Smo by Smurf family of E3 ubiquitin ligases [34].

Finally, the main goal of this study was to investigate whether Hh co-receptors may be used to modulate Hh signaling in ECs for therapeutical purposes. By identifying Cdon as a negative regulator of Dhh in ECs, and by demonstrating that Cdon KO prevents BBB opening in the setting of brain inflammation, the present study offer the possibility of using Cdon blocking molecules including blocking antibodies (Figure 6G-H) as therapeutic tools to preserve endothelial integrity at least in the setting of inflammation. Notably, inflammatory cytokines including TNFα and Il1β increase Cdon expression in ECs.

Acknowledgment,

We thank Carnegie for proving with the Gas1 Floxed mice. We thank Annabel Reynaud, Sylvain Grolleau, and Maxime David for their technical help. We thank Christelle Boullé for administrative assistance.

Sources of funding

This study was supported by grants from the Fondation de France (Appel d'Offre Recherche sur les maladies Cardiovasculaires 2013 and 2018), the Fondation pour la Recherche Médicale (équipe FRM) and the Fondation ARSEP pour la recherche sur la sclérose en plaques. Also this study was funded by a Marie Skłodowska-Curie Actions (MSCA-IF-2019) from the European concil. Finally, this study was co-funded by the "Institut National de la Santé et de la Recherche Médicale" and by the University of Bordeaux.

Disclosure

None

References

1. Peng Z, Shu B, Zhang Y, Wang M. Endothelial Response to Pathophysiological Stress. *Arterioscler Thromb Vasc Biol*. 2019;39:e233-e243.

2. Chapouly C, Guimbal S, Hollier P-L, Renault M-A. Role of Hedgehog Signaling in Vasculature Development, Differentiation, and Maintenance. *Int J Mol Sci*. 2019;20. 3076

3. Alvarez JI, Dodelet-Devillers A, Kebir H, Ifergan I, Fabre PJ, Terouz S, Sabbagh M, Wosik K, Bourbonniere L, Bernard M, van Horssen J, de Vries HE, Charron F, Prat A. The Hedgehog pathway promotes blood-brain barrier integrity and CNS immune quiescence. *Science*. 2011;334:1727-1731.

4. Xia YP, He QW, Li YN, Chen SC, Huang M, Wang Y, Gao Y, Huang Y, Wang MD, Mao L, Hu B. Recombinant human sonic hedgehog protein regulates the expression of ZO-1 and occludin by activating angiopoietin-1 in stroke damage. *PloS one*. 2013;8:e68891.

5. Chapouly C, Yao Q, Vandierdonck S, Larrieu-Lahargue F, Mariani JN, Gadeau AP, Renault MA. Impaired Hedgehog signalling-induced endothelial dysfunction is sufficient to induce neuropathy: implication in diabetes. *Cardiovascular research*. 2016;109:217-227.

6. Caradu C, Couffinhal T, Chapouly C, Guimbal S, Hollier P-L, Ducasse E, Bura-Rivière A, Dubois M, Gadeau A-P, Renault M-A. Restoring Endothelial Function by Targeting Desert Hedgehog Downstream of Klf2 Improves Critical Limb Ischemia in Adults. *Circ Res*. 2018;123:1053-1065.

7. Hollier P-L, Guimbal S, Mora P, Diop A, Cornuault L, Couffinhal T, Gadeau A-P, Renault M-A, Chapouly C. Genetic disruption of the Blood Brain Barrier leads to protective barrier formation at the Glia Limitans. *bioRxiv*. doi:10.1101/2020.03.13.990762

8. Lehmann GL, Hanke-Gogokhia C, Hu Y, Bareja R, Salfati Z, Ginsberg M, Nolan DJ, Mendez-Huergo SP, Dalotto-Moreno T, Wojcinski A, Ochoa F, Zeng S, Cerliani JP, Panagis L, Zager PJ, Mullins RF, Ogura S, Lutty GA, Bang J, Zippin JH, Romano C, Rabinovich GA, Elemento O, Joyner AL, Rafii S, Rodriguez-Boulan E, Benedicto I. Single-cell profiling reveals an endothelium-mediated immunomodulatory pathway in the eye choroid. *J Exp Med*. 2020;217.

9. Dakubo GD, Mazerolle C, Furimsky M, Yu C, St-Jacques B, McMahon AP, Wallace VA. Indian hedgehog signaling from endothelial cells is required for sclera and retinal pigment epithelium development in the mouse eye. *Developmental biology*. 2008;320:242-255.

10. Hollier P-L, Chapouly C, Diop A, Guimbal S, Cornuault L, Gadeau A-P, Renault M-A. Endothelial cell response to Hedgehog ligands depends on their processing. *bioRxiv*. doi:10.1101/2020.03.03.974444

11. Nusslein-Volhard C, Wieschaus E. Mutations affecting segment number and polarity in Drosophila. *Nature*. 1980;287:795-801.

12. Robbins DJ, Fei DL, Riobo NA. The Hedgehog signal transduction network. *Science signaling*. 2012;5:re6.

13. Ramsbottom SA, Pownall ME. Regulation of Hedgehog Signalling Inside and Outside the Cell. *J Dev Biol*. 2016;4.

14. Sanchez-Arrones L, Cardozo M, Nieto-Lopez F, Bovolenta P. Cdon and Boc: Two transmembrane proteins implicated in cell-cell communication. *Int J Biochem Cell Biol*. 2012;44:698-702.

15. Lee CS, Buttitta L, Fan CM. Evidence that the WNT-inducible growth arrest-specific gene 1 encodes an antagonist of sonic hedgehog signaling in the somite. *Proceedings of the National Academy of Sciences of the United States of America*. 2001;98(20):11347-11352.

16. Jin S, Martinelli DC, Zheng X, Tessier-Lavigne M, Fan CM. Gas1 is a receptor for sonic hedgehog to repel enteric axons. *Proceedings of the National Academy of Sciences of the United States of America*. 2015;112:E73-80.

17. Azzoni E, Conti V, Campana L, Dellavalle A, Adams RH, Cossu G, Brunelli S. Hemogenic endothelium generates mesoangioblasts that contribute to several mesodermal lineages in vivo. *Development*. 2014;141:1821-1834.

18. Kenyon BM, Voest EE, Chen CC, Flynn E, Folkman J, D'Amato RJ. A model of angiogenesis in the mouse cornea. *Investigative ophthalmology & visual science*. 1996;37:1625-1632.

19. Horng S, Therattil A, Moyon S, Gordon A, Kim K, Argaw AT, Hara Y, Mariani JN, Sawai S, Flodby P, Crandall ED, Borok Z, Sofroniew MV, Chapouly C, John GR. Astrocytic tight junctions control inflammatory CNS lesion pathogenesis. *J Clin Invest*. 2017;127:3136-3151.

20. Argaw AT, Gurfein BT, Zhang Y, Zameer A, John GR. VEGF-mediated disruption of endothelial CLN-5 promotes blood-brain barrier breakdown. *Proc Natl Acad Sci USA*. 2009;106:1977-1982.

21. Agrawal V, Kim DY, Kwon YG. Hhip regulates tumor-stroma-mediated upregulation of tumor angiogenesis. *Experimental & molecular medicine*. 2017;49:e289.

22. Sekiguchi H, Ii M, Jujo K, Renault MA, Thorne T, Clarke T, Ito A, Tanaka T, Klyachko E, Tabata Y, Hagiwara N, Losordo DW. Estradiol Triggers Sonic-hedgehog-induced Angiogenesis During Peripheral Nerve Regeneration by Downregulating Hedgehog-interacting Protein. *Lab Invest*. 2012;92:532-542

23. Nie DM, Wu QL, Zheng P, Chen P, Zhang R, Li BB, Fang J, Xia LH, Hong M. Endothelial microparticles carrying hedgehog-interacting protein induce continuous endothelial damage in the pathogenesis of acute graft-versus-host disease. *Am J Physiol Cell Physiol*. 2016;310:C821-35.

24. Wang Y, Alexander JS. Analysis of endothelial barrier function in vitro. *Methods Mol Biol*. 2011;763:253-264.

25. Cardozo MJ, Sanchez-Arrones L, Sandonis A, Sanchez-Camacho C, Gestri G, Wilson SW, Guerrero I, Bovolenta P. Cdon acts as a Hedgehog decoy receptor during proximal-distal patterning of the optic vesicle. *Nature communications*. 2014;5:4272.

26. Casillas C, Roelink H. Gain-of-function Shh mutants activate Smo cell-autonomously independent of Ptch1/2 function. *Mech Dev*. 2018;153:30-41.

27. Allen BL, Song JY, Izzi L, Althaus IW, Kang J-S, Charron F, Krauss RS, McMahon AP. Overlapping roles and collective requirement for the coreceptors GAS1, CDO, and BOC in SHH pathway function. *Dev Cell*. 2011;20:775-787.

28. Renault MA, Roncalli J, Tongers J, Thorne T, Klyachko E, Misener S, Volpert OV, Mehta S, Burg A, Luedemann C, Qin G, Kishore R, Losordo DW. Sonic hedgehog induces angiogenesis via Rho kinase-dependent signaling in endothelial cells. *Journal of molecular and cellular cardiology*. 2010;49:490-498.

29. Chinchilla P, Xiao L, Kazanietz MG, Riobo NA. Hedgehog proteins activate pro-angiogenic responses in endothelial cells through non-canonical signaling pathways. *Cell cycle (Georgetown, Tex*. 2010;9:570-579.

30. Lee CS, Buttitta L, Fan CM. Evidence that the WNT-inducible growth arrest-specific gene 1 encodes an antagonist of sonic hedgehog signaling in the somite. *Proc Natl Acad Sci USA*. 2001;98:11347-11352.

31. Martinelli DC, Fan CM. Gas1 extends the range of Hedgehog action by facilitating its signaling. *Genes & development*. 2007;21:1231-1243.

32. Tenzen T, Allen BL, Cole F, Kang JS, Krauss RS, McMahon AP. The cell surface membrane proteins Cdo and Boc are components and targets of the Hedgehog signaling pathway and feedback network in mice. *Dev Cell*. 2006;10:647-656.

33. Zhang W, Kang J-S, Cole F, Yi M-J, Krauss RS. Cdo functions at multiple points in the Sonic Hedgehog pathway, and Cdo-deficient mice accurately model human holoprosencephaly. *Dev Cell*. 2006;10:657-665.

34. Li S, Li S, Wang B, Jiang J. Hedgehog reciprocally controls trafficking of Smo and Ptc through the Smurf family of E3 ubiquitin ligases. *Sci Signal*. 2018;11.

Highlights

- Gas1 and Cdon are differentially regulated by inflammatory cytokines and modulate Dhh effects in endothelial cells
- Gas1 promotes Dhh-induced endothelial immune quiescence by promoting Dhh interaction with Smo
- Cdon prevents Dhh binding to Ptch1 and by doing so, destabilizes endothelial adherens junctions and promotes angiogenesis.
- Cdon blocking molecules may be used to preserve endothelium integrity especially at the blood brain barrier in the setting of neuroinflammation.

Figures and Legends to Figures

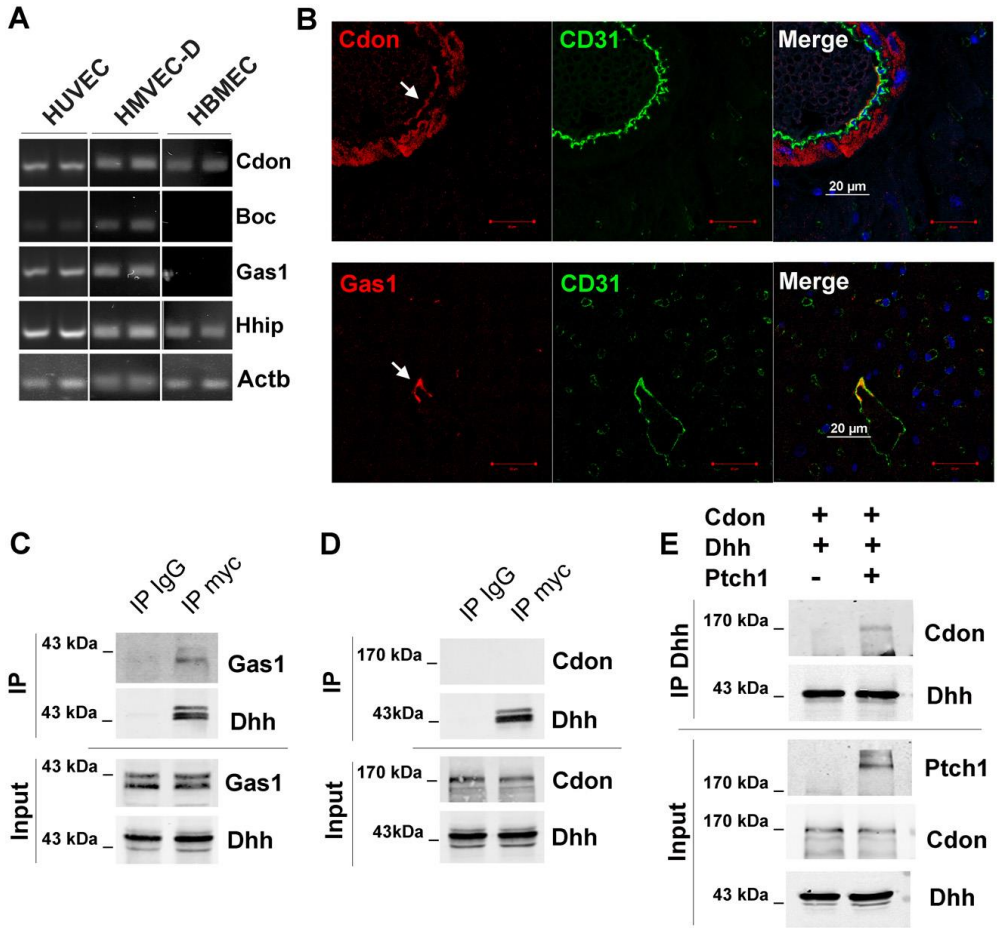

Figure 1: ECs express Cdon, Gas1 and Hhip. (**A**) *Cdon*, *Boc*, *Gas1*, *Hhip* and *Actb* mRNA expression was evaluated via RT-PCR in HUVECs, HMVECs-D and HBMECs. (**B**) Heart cross section from wild type mice were co-immunostained with anti-Cdon (in red) or anti-Gas1 (in red) antibodies together with anti-CD31 (in green) antibodies to identify Cdon or Gas1 expression in ECs respectively. (**C**) HeLa were co-transfected with Gas1 and myc-tagged Dhh encoding vectors. Gas1 interaction with Dhh was evaluated by co-immunoprecipitation assay. (**D**) HeLa were co-transfected with Cdon and myc-tagged Dhh encoding vectors. Cdon interaction with Dhh was evaluated by co-immunoprecipitation assay. (**E**) HeLa were co-transfected with Cdon, Ptch1 and Dhh encoding vectors. Cdon interaction with Dhh was evaluated by co-immunoprecipitation assay.

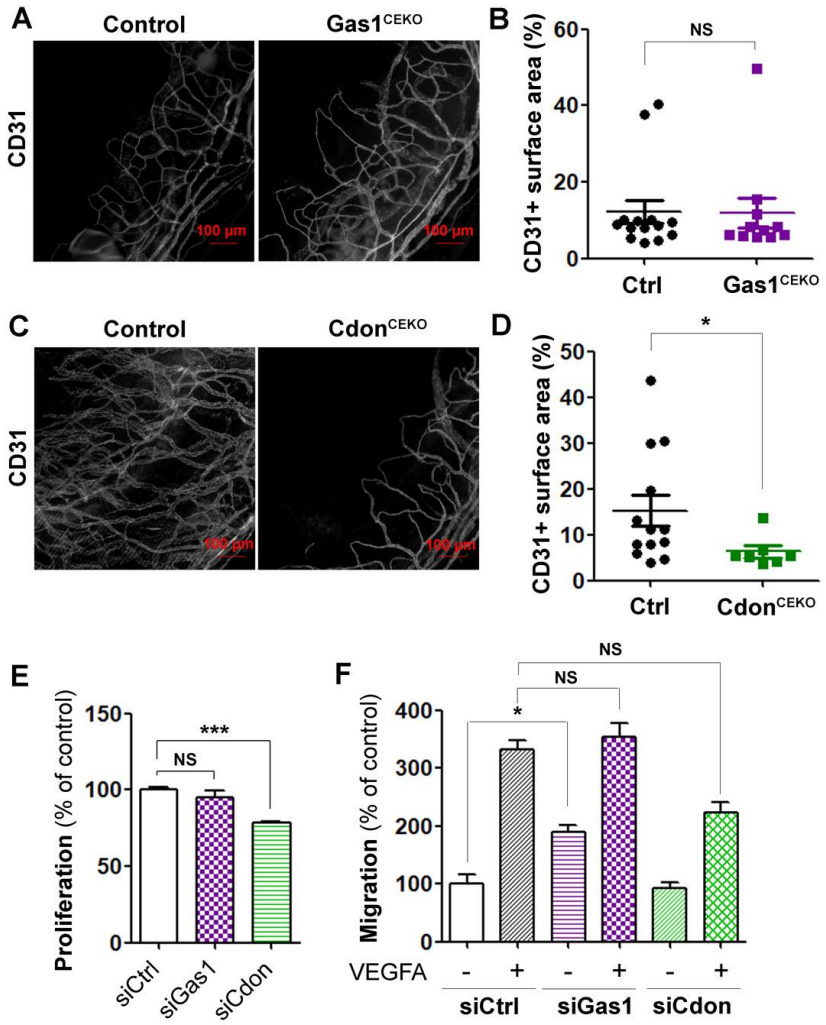

Figure 2: Cdon promotes EC migration, proliferation and angiogenesis. (**A-B)** VEGFA containing pellets were implanted in the corneas of Cdh5-Cre/ERT2 *Gas1*$^{Flox/Flox}$ (*Gas1*^{ECKO}) and *Gas1*$^{Flox/Flox}$ (control) mice 2 week after they were administered with tamoxifen (n=14 and 11 corneas respectively). (**A**) Whole mount corneas were immunostained with anti-CD31 antibodies to identify blood vessels. Representative pictures are shown. (**B**) Angiogenesis was quantified as the percentage of CD31+ surface area. (**C-D)** VEGFA containing pellets were implanted in the corneas of Cdh5-Cre/ERT2; *Cdon*$^{Flox/Flox}$ (*Cdon*^{ECKO}) and *Cdon*$^{Flox/Flox}$ (control) mice 2 week after they were administered with tamoxifen (n=13 and 7 corneas respectively). (**C**) Whole mount corneas were immunostained with anti-CD31 antibodies to identify blood vessels. Representative pictures are shown. (**D**) Angiogenesis was quantified as the percentage of CD31+ surface area. (**E-F**) HUVECs were transfected with *Gas1*, *Cdon* or control siRNAs. (**E**) Cells proliferation was assessed using MTT. The experiment was repeated 3 times, each experiment included n=8 wells/condition. (**F**) Cell migration was assessed in a chemotaxis chamber in the presence or not of 50 ng/mL VEGFA. The experiment was repeated 3 times, each experiment included n=4 wells/condition. *: p≤0.05; **: p≤0.01; ***: p≤0.001. NS: not significant. Mann Whitney test or Kruskal-Wallis test followed by Dunn's multiple comparisons test.

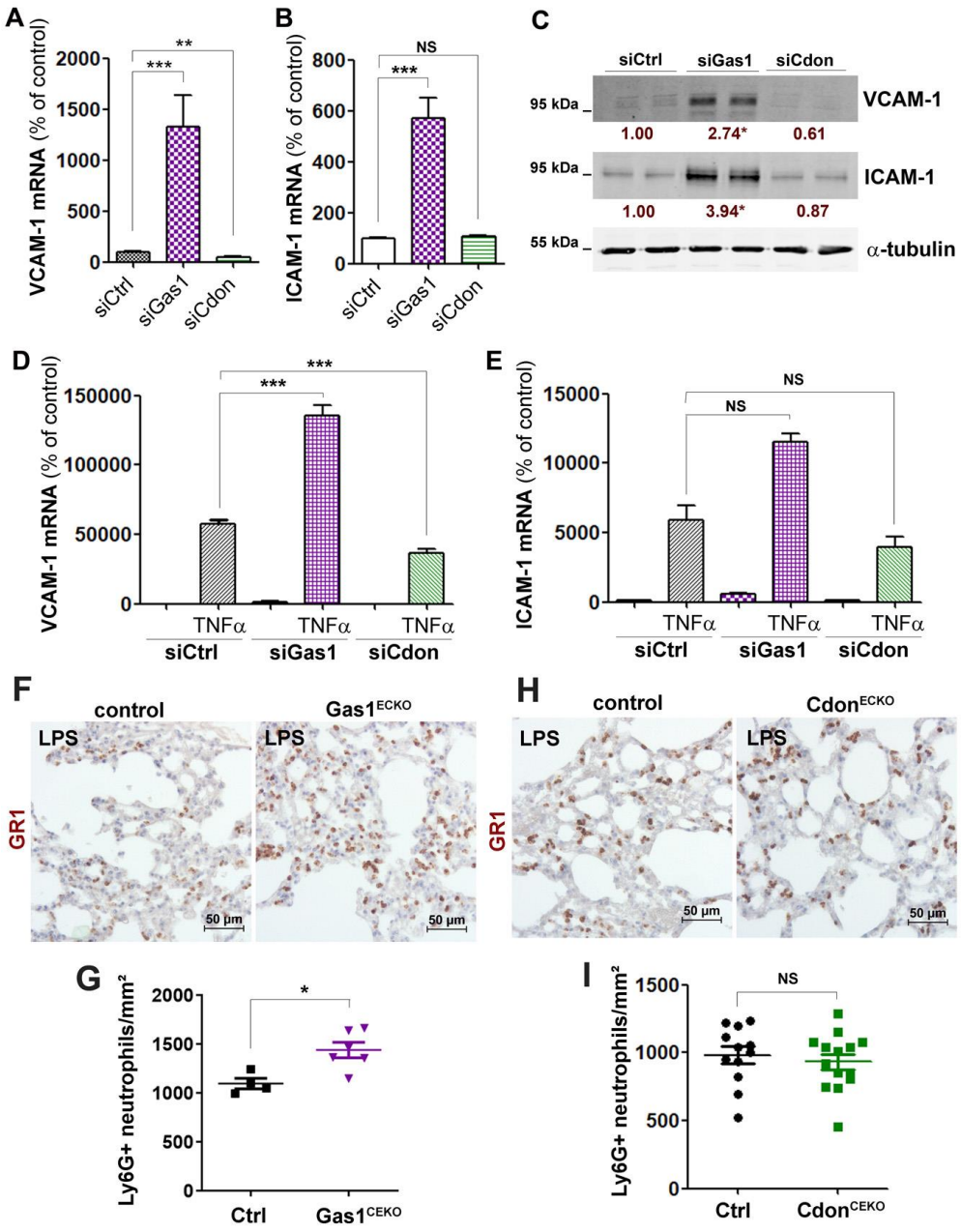

Figure 3: Gas1 prevents EC activation and neutrophil recruitment. (**A-C**) HUVECs were transfected with *Gas1*, *Cdon* or control siRNAs. *VCAM-1* (**A**) and *ICAM-1* (**B**) mRNA expression was quantified via RT-qPCR. The experiment was repeated 3 times, each experiment included triplicates. (**C**) VCAM-1 and ICAM-1 protein expression was quantified by western blot analysis the experiment was repeated at least 3 times, each experiment included duplicates. (**D-E**) HUVECs were transfected with *Gas1*, *Cdon* or control siRNAs and then treated or not with 10 ng/mL TNFα for 6 hours. *VCAM-1* (**D**) and *ICAM-1* (**E**) mRNA expression was quantified via RT-qPCR. The experiment was repeated 3 times, each experiment included triplicates. (**F-G**) Cdh5-Cre/ERT2 $Gas1^{Flox/Flox}$ ($Gas1^{ECKO}$) and $Gas1^{Flox/Flox}$ (control) mice were treated with 10 mg/kg LPS and sacrificed 6 hours later. (**F**) Lung sections were immunostained with anti-Ly6G (GR1) antibodies to identify neutrophils. (**G**) Neutrophil infiltration was quantified as the number of Ly6G+ cells/mm² (n=5 and 6 respectively). (**H-I**) Cdh5-Cre/ERT2 $Cdon^{Flox/Flox}$ ($Cdon^{ECKO}$) and $Cdon^{Flox/Flox}$ (control) mice were treated with 10 mg/kg LPS and sacrificed 6 hours later. (**H**) Lung sections were

immunostained with anti-Ly6G (GR1) antibodies to identify neutrophils. (**I**) Neutrophil infiltration was quantified as the number of Ly6G+ cells/mm² (n=14 and 12 respectively). *: p≤0.05; ***: p≤0.001. NS: not significant. Mann Whitney test or Kruskal-Wallis test followed by Dunn's multiple comparisons test.

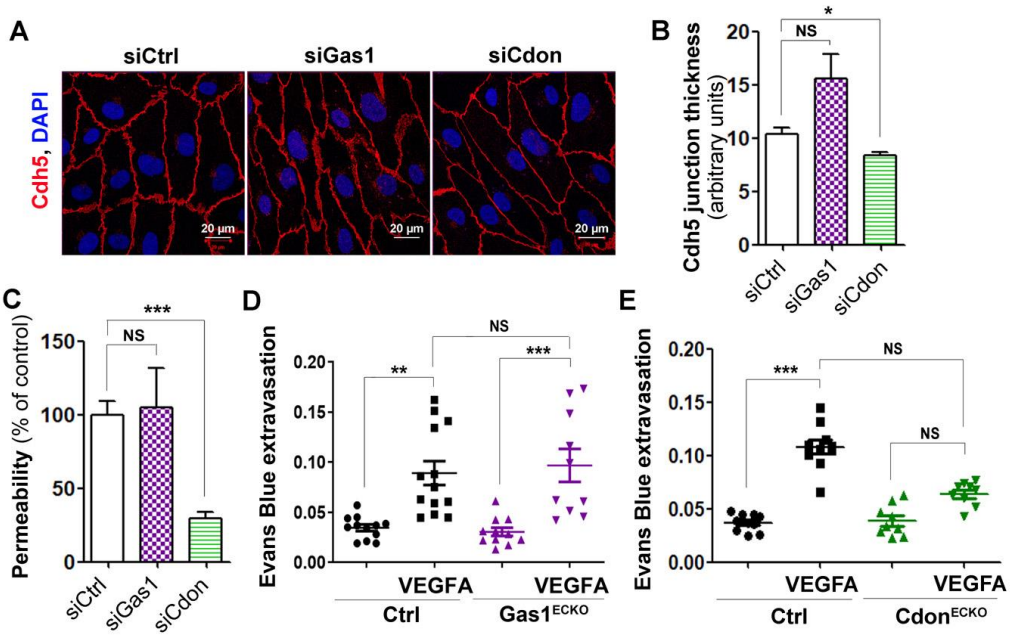

Figure 4: Gas1 promotes adherens junction integrity while Cdon disrupts it. (**A-C**) HUVECs were transfected with *Gas1*, *Cdon* or control siRNAs. (**A**) Cdh5 localization was evaluated by immunofluorescent staining (in white) of a confluent cell monolayer and (**B**) quantified as the mean junction thickness using Image J software. The experiment was repeated at least 4 times. (**C**) Endothelial monolayer permeability to 70 kDa FITC-Dextran was assessed using Transwells. The experiment was repeated 3 times, each experiment included duplicates. (**D**) VEGFA-induced permeability was assessed in both Cdh5-Cre/ERT2 *Gas1*$^{Flox/Flox}$ (*Gas1*^{ECKO}) and *Gas1*$^{Flox/Flox}$ (control) mice using the Miles assay (n=10 and 14 mice respectively). (**E**) VEGFA-induced permeability was assessed in both Cdh5-Cre/ERT2; *Cdon*$^{Flox/Flox}$ (*Cdon*^{ECKO}) and *Cdon*$^{Flox/Flox}$ (control) mice using the Miles assay (n=9 and 10 mice respectively). *: p≤0.05; **: p≤0.01; ***: p≤0.001. NS: not significant. Kruskal-Wallis test followed by Dunn's multiple comparisons test.

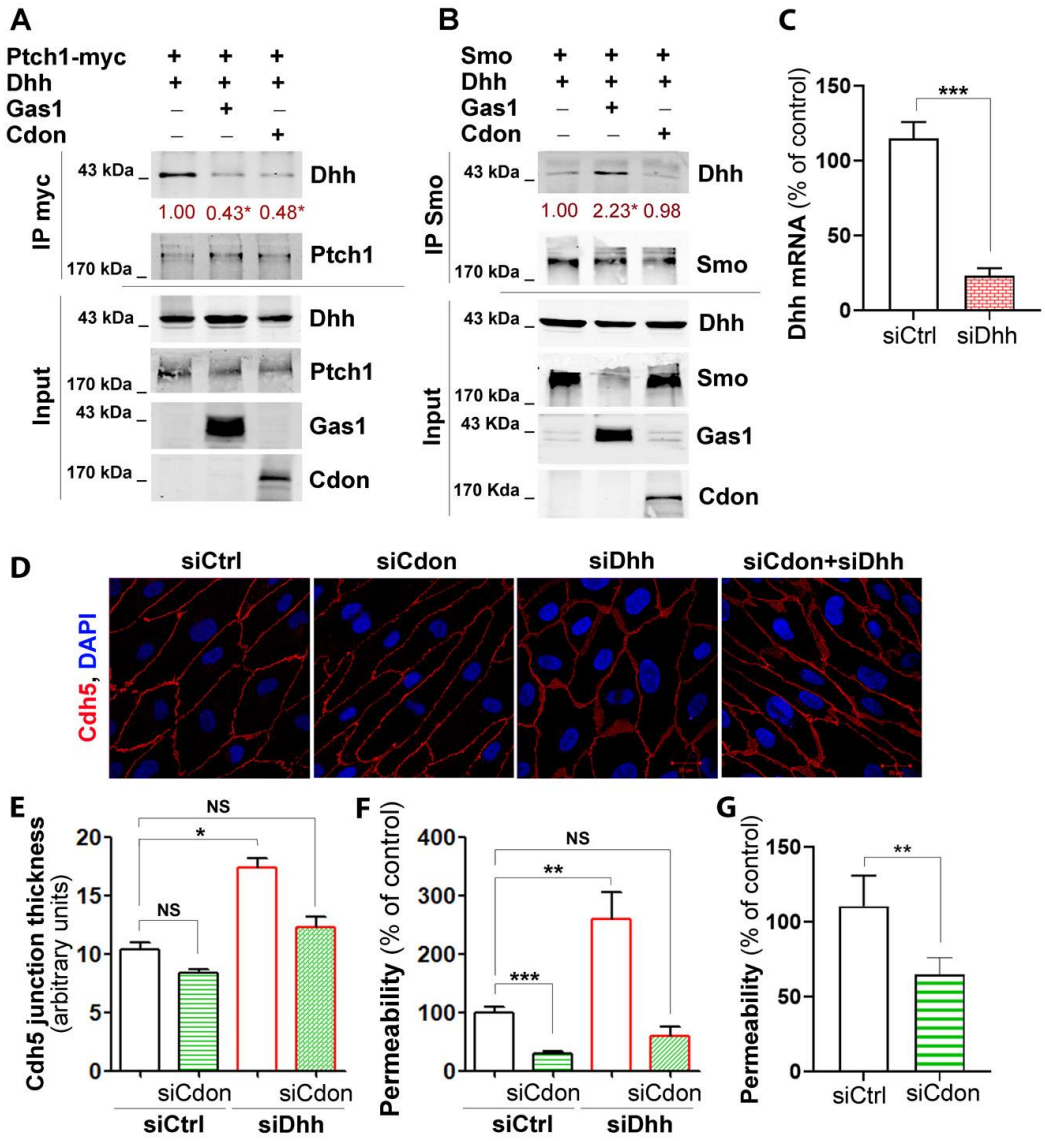

Figure 5: Gas1 promotes Dhh binding to Smo while Cdon prevents Dhh binding to Ptch1. (**A**) HeLa were co-transfected by Ptch1-myc and Dhh encoding plasmids together with or without Gas1 or Cdon encoding plasmids. Dhh interaction with Ptch1 was assessed by co-immunoprecipitation assay. The experiment was repeated 4 times. (**B**) HeLa were co-transfected Smo and Dhh encoding plasmids together with or without Gas1 or Cdon encoding plasmids. Dhh interaction with Smo was assessed by co-immunoprecipitation assay. The experiment was repeated 4 times. (**C**) HUVECs were transfected with *Dhh* or control siRNAs. Dhh mRNA expression was measured via RT-qPCR. The experiment was repeated 3 times, each experiment included triplicates. (**D-F**) HUVECs were co-transfected with *Cdon* or control siRNAs together with or without *Dhh* siRNAs. (**D**) Cdh5 localization was evaluated by immunofluorescent staining (in white) of a confluent cell monolayer and (**E**) quantified as the mean junction thickness using Image J software. The experiment was repeated at least 4 times. (**F**) Endothelial monolayer permeability to 70 kDa FITC-Dextran was assessed using Transwells. The experiment was repeated 3 times, each experiment included duplicates. (**G**) HUVECs were transfected with *Dhh* or control siRNAs. Endothelial monolayer permeability to 70 kDa FITC-Dextran was assessed using Transwells in serum-free conditions. The experiment was repeated 3 times, each experiment included duplicates.

*: p≤0.05; **: p≤0.01; ***: p≤0.001. NS: not significant. Kruskal-Wallis test followed by Dunn's multiple comparisons test.

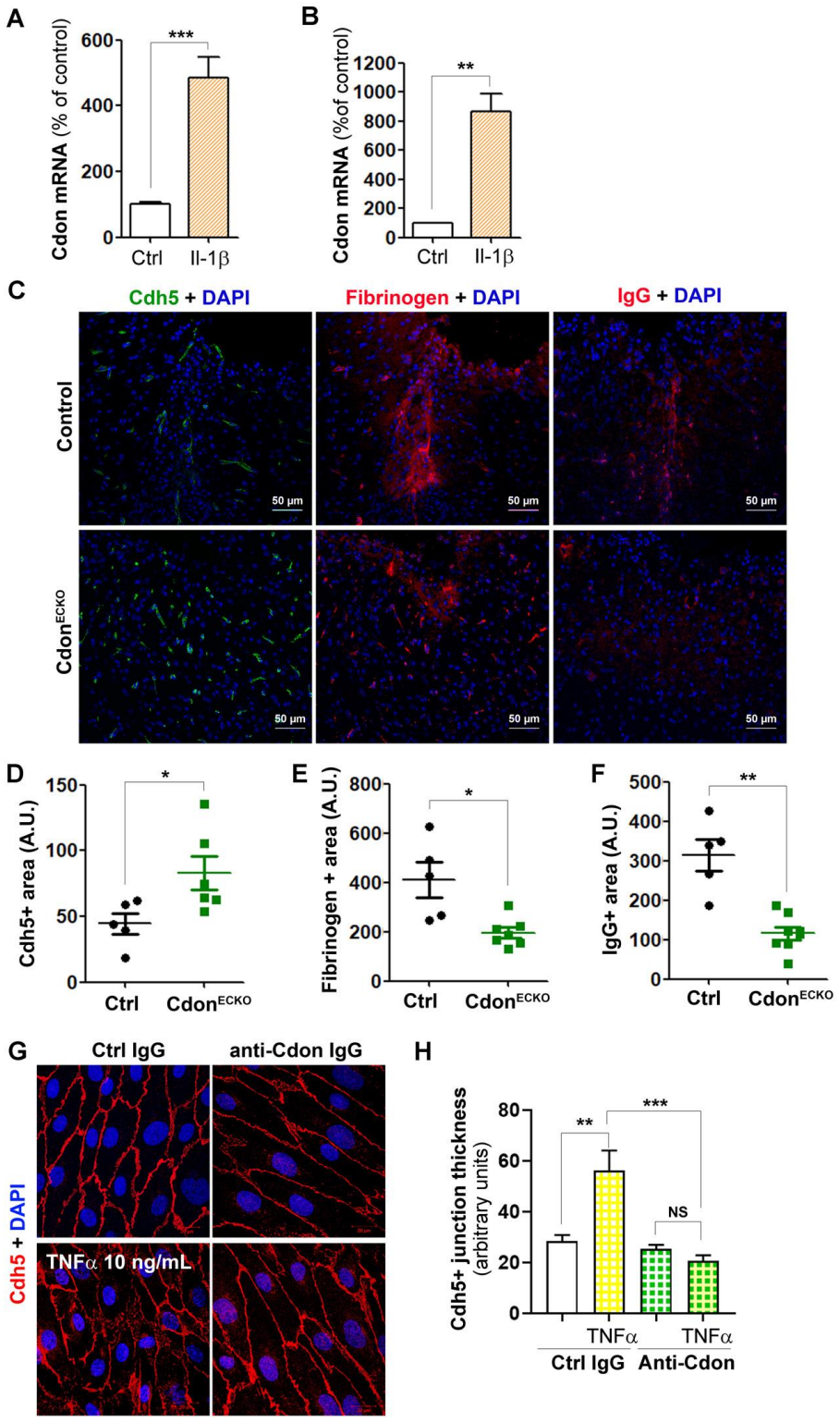

Figure 6: Cdon deficiency in ECs prevents Il1β-induced BBB disruption. HUVECs (**A**) and HBMECs (**B**) were treated or not with 10 ng/mL Il1β for 6 hours. Cdon mRNA expression was quantified via RT-qPCR. Experiments were repeated 3 times, each experiment included triplicates. (**C-F**) Both Cdh5-Cre/ERT2; *Cdon*$^{Flox/Flox}$ (*Cdon*^{ECKO}) and *Cdon*$^{Flox/Flox}$ (control) mice were administered in the cerebral cortex with adenoviruses encoding Il-1β (n=7 and 5 mice respectively). Mice were sacrificed 7 days later. (**C**) Brain sagittal sections were

immunostained with anti-Cdh5 (in green), anti-fibrinogen (in red) or anti-IgG (in red) antibodies. Representative confocal images are shown. (**D**) Cdh5 expression was quantified as the Cdh5+ surface area. (**E**) Fibrinogen extravasation was quantified as the fibrinogen+ surface area. (**F**) IgG extravasation was quantified as the IgG+ surface area. **(G-H)** HUVECs were treated or not with 10 ng/mL TNFα in the presence of 1.5 µg/mL Cdon blocking antibodies or 1.5 µg/mL unspecific IgGs for 2 hours. (**G**) Cdh5 localization was evaluated by immunofluorescent staining (in red) of a confluent cell monolayer and (**B**) quantified as the mean junction thickness using Image J software. The experiment was repeated at least 4 times. *: p≤0.05; **: p≤0.01; ***: p≤0.001. NS: not significant. Mann Withney test or one way ANOVA followed by Bonferroni's multiple comparisons test.